Correction of mutations within the cystic fibrosis transmembrane conductance regulator by site-directed RNA editing

Maria Fernanda Montiel-Gonzalez[a,b], Isabel Vallecillo-Viejo[a,c], Guillermo A. Yudowski[a,d], and Joshua J. C. Rosenthal[a,b,1]

[a]Institute of Neurobiology, University of Puerto Rico-Medical Sciences Campus, San Juan, Puerto Rico 00901; and [b]Department of Biochemistry, [c]Department of Pharmacology, and [d]Department of Anatomy and Neurobiology, University of Puerto Rico-Medical Sciences Campus, San Juan, Puerto Rico 00936

Edited by Lily Yeh Jan, University of California, San Francisco, CA, and approved September 19, 2013 (received for review April 3, 2013)

Adenosine deaminases that act on RNA are a conserved family of enzymes that catalyze a natural process of site-directed mutagenesis. Biochemically, they convert adenosine to inosine, a nucleotide that is read as guanosine during translation; thus when editing occurs in mRNAs, codons can be recoded and the changes can alter protein function. By removing the endogenous targeting domains from human adenosine deaminase that acts on RNA 2 and replacing them with an antisense RNA oligonucleotide, we have engineered a recombinant enzyme that can be directed to edit anywhere along the RNA registry. Here we demonstrate that this enzyme can efficiently and selectively edit a single adenosine. As proof of principle in vitro, we correct a premature termination codon in mRNAs encoding the cystic fibrosis transmembrane conductance regulator anion channel. In *Xenopus* oocytes, we show that a genetically encoded version of our editase can correct cystic fibrosis transmembrane conductance regulator mRNA, restore full-length protein, and reestablish functional chloride currents across the plasma membrane. Finally, in a human cell line, we show that a genetically encoded version of our editase and guide RNA can correct a nonfunctional version of enhanced green fluorescent protein, which contains a premature termination codon. This technology should spearhead powerful approaches to correcting a wide variety of genetic mutations and fine-tuning protein function through targeted nucleotide deamination.

RNA editing by adenosine deamination is an epigenetic process used by all metazoans to precisely change genetic information. Catalyzed by the adenosine deaminases that act on RNA (ADAR) family of enzymes, adenosines are converted to inosine in a wide variety of RNAs (1–6). When editing occurs in coding regions of mRNAs, inosine is read as guanosine (7), often causing codons to change in a process that resembles a natural system for site-directed mutagenesis. As expected from a mechanism that can recode almost half of all codons, the effects of RNA editing on protein function are diverse (8). The best-studied examples come from mRNAs encoding elements of the machinery for excitability in the nervous system, where editing changes ion selectivity of ionotropic glutamate receptors, G-protein coupling of metabotropic serotonin receptors, inactivation of a voltage-dependent K^+ channel, and the transport rate of a Na^+/K^+ ATPase, among other things (9–12). Because of its versatility, the ability to control RNA editing could prove useful for medicine and basic research. For example, mutations that cause premature termination codons (UAA, UGA, UAG) could be recoded to tryptophan (UGG). Perhaps more importantly, protein function itself could be tuned. The key to realizing this potential lies in the ability to manipulate ADAR's targeting.

ADARs are modular enzymes, containing distinct domains that perform different functions (13). At their C terminus, they contain a deaminase domain that catalyzes the hydrolytic deamination of adenosine to inosine. At their N terminus lie a variable number of double-stranded RNA-binding motifs (dsRBMs), highly conserved structures that bind both perfect and imperfect RNA duplexes. To edit a specific adenosine, ADAR's dsRBMs bind surrounding structures, often formed between intronic and exonic sequences in pre-mRNAs. The structures can be complex, composed of imperfect stems, bulges, and loops, and may require primary sequences separated by kilobases (14, 15). This necessity for intricate *cis*-acting elements renders ADAR's endogenous targeting mechanism difficult to manipulate. We reasoned that an antisense RNA oligonucleotide would provide a more flexible targeting domain because it could be designed to bind any primary sequence. Thus, our strategy was to replace ADAR's dsRBMs with an antisense RNA oligonucleotide to guide the catalytic activity to any specific address along an RNA.

At the outset, our strategy raised several questions. First, would the isolated deaminase domain retain significant catalytic activity? An earlier study demonstrated that it was able to edit at a low level, consistent with the idea that it retained its ability to deaminate but lacked the means to efficiently bind a substrate (16). Another issue was whether a deaminase domain that lacked dsRBMs would still require double-stranded RNA. Finally, the most pressing question was how to connect an RNA oligonucleotide to the deaminase domain. The nature of this coupling was a critical consideration for the overall utility of site-directed RNA editing. Although chemical reactions could be used to link the two elements, most had the disadvantage of requiring a reaction in vitro. This would hamper future strategies for delivery, necessitating the transport of a large riboprotein complex across cell membranes. Furthermore, the cargo could not be further amplified by the cellular machinery. A better strategy would be to deliver the catalytic domain and the guide RNA as separate, genetically encoded elements that could link once expressed in the cell. In this report we show that, when fused to a small

Significance

RNA editing by adenosine deamination is a natural process of site-directed mutagenesis used by organisms to modify genetic information as it passes through RNA. In this paper we present an engineered RNA editing enzyme that can be induced to edit any adenosine that is chosen. We show that our system can efficiently correct a premature stop codon in the cystic fibrosis transmembrane conductance regulator in frog oocytes. Furthermore, a fully genetically encoded version of the system functions in human cells. As a general method, site-directed RNA editing could be a useful technique for correcting genetic mutations and modifying protein function.

Author contributions: M.F.M.-G. and J.J.C.R. designed research; M.F.M.-G., I.V.-V., G.A.Y., and J.J.C.R. performed research; G.A.Y. contributed new reagents/analytic tools; M.F.M.-G., I.V.-V., and J.J.C.R. analyzed data; and M.F.M.-G. and J.J.C.R. wrote the paper.

The authors declare no conflict of interest.

This article is a PNAS Direct Submission.

[1]To whom correspondence should be addressed. E-mail: joshua.rosenthal@upr.edu.

This article contains supporting information online at www.pnas.org/lookup/suppl/doi:10.1073/pnas.1306243110/-/DCSupplemental.

λ-phage RNA-binding protein, ADAR's deaminase domain can be coupled to an antisense RNA oligonucleotide inside a cell and that the complex can guide site-specific mRNA editing and correct premature termination.

Results

Engineering a Site-Directed RNA Editase. Our overall strategy for generating a site-directed editase was to link human ADAR2's deaminase domain to an antisense guide oligonucleotide through an interaction that could be genetically encoded. With this in mind, we looked for an RNA-binding protein that recognizes a specific RNA sequence. The RNA-binding protein would be linked to ADAR's deaminase domain, and the sequence that the protein recognizes would be linked to an antisense RNA guide oligonucleotide. A useful binding interaction would require two key features: First, the interacting partners should be small so that they do not interfere with the function of the deaminase domain or the guide. Second, they should bind with a high affinity to drive the editing process in the complex cellular environment. The λ-phage N protein-boxB RNA interaction, which normally regulates antitermination during transcription of λ-phage mRNAs, fits these criteria (17). The λN peptide, which mediates the binding of the N protein, is only 22 amino acids long, and the boxB RNA hairpin that it recognizes is only 17 nucleotides long and they can bind with nanomolar affinity (18). To generate a recombinant editase, the λN peptide was fused to the deaminase domain of human ADAR2 (λN–DD), and recombinant protein was purified from the yeast *Pichia pastoris* as previously described (19, 20). Filter binding assays between λN–DD and a ^{32}P-labeled boxB RNA oligonucleotide demonstrated that the λN peptide retained a high affinity for boxB when coupled to ADAR's deaminase domain (17 ± 2.5 nM, $n = 5$; Fig. S1). The first questions that we posed were whether the deaminase domain is active on its own, and, if so, can it be guided to a specific region of an RNA by an antisense RNA oligonucleotide coupled via the λN-boxB interaction?

Site-Directed RNA Editase Is Active and Can Be Guided by an Antisense RNA. To test λN–DD's activity, and whether the λ*N*–DD:boxB interaction is required for editing, we took advantage of a recombinant RNA that contained four boxB hairpins (21) (Fig. 1*A*; note that this is the only experiment where boxB was inserted into the target RNA; in all other experiments, it is inserted into the guide oligonucleotide). For this experiment, we designed an antisense oligonucleotide complementary to sequence adjacent to two of the four boxB hairpins. 4boxB RNA and the guide oligonucleotide were incubated in vitro with λN–DD. 4boxB RNA was then converted to cDNA, amplified by PCR, and directly sequenced. Fig. 1*B* shows an example of three adenosines that were efficiently converted to inosine, whereas the no-enzyme control showed no evidence of conversion. In total, five adenosines were edited at efficiencies ranging from 50 to 100% (Fig. 1*C*). Within the 344 nt analyzed for editing in our RT-PCR product, no other adenosines were edited. All conversions were in sequence complementary to the antisense oligonucleotide, suggesting that double-stranded RNA is required for the deaminase domain to edit. Control experiments showed that almost all editing at four of the five sites could be blocked by an excess of free boxB hairpin RNA. However, an excess of free boxB hairpin RNA that contained two mutations known to disrupt its binding to the λN peptide did not block editing (22, 23). At position 2, editing was greatly reduced, but not completely abolished, by an excess of boxB hairpin. This adenosine may already exist within a structure that can promote editing, albeit poorly. At all five positions, an excess of λN peptide blocked editing completely. These results showed that the λN-boxB interaction is required for editing, and we conclude that robust editing can be driven in a *cis*-strand by λN–DD.

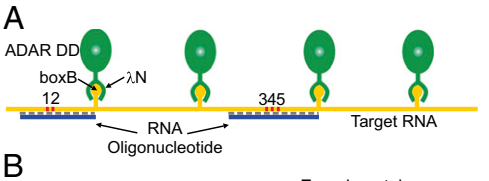

C

TREATMENT	EDITING PERCENTAGE site 1	site 2	site 3	site 4	site 5
Experimental	51±2.4	94±0.5	73±0.8	84±0.7	94±0.5
No λN	NE	NE	NE	NE	NE
No RNA Oligo	NE	23±1.2	NE	NE	7±0.7
Excess λN	NE	NE	NE	NE	NE
Excess boxB	NE	22±0.5	NE	NE	7±0.4
Excess mut. boxB	43±4.1	84±2.4	80±1.1	92±0.4	98±0.4

Fig. 1. Recombinant λN–DD is catalytically active and requires boxB to edit. (*A*) A schematic of the experimental design. After incubating 4boxB target RNA with λN–DD and a complementary antisense RNA oligonucleotide, RT-PCR revealed editing at five adenosines (1–5, in red). (*B*) Electropherograms showing editing at adenosines 3–5 (asterisks). (*C*) Editing percentages at sites 1–5 under experimental and control conditions. λN peptide, boxB oligo, and a mutant boxB oligo (G8A, A10C) that does not bind the λN peptide were added as blockers to the reaction. "NE" indicates no editing was evident. Editing percentages were quantified using the relative peak heights from antisense direct-sequencing electropherograms of RT-PCR products. $n = 3 \pm$ SEM.

Results thus far supported the idea that boxB could tether editing to a specific region. Next, we asked if it could couple λN–DD to an antisense oligonucleotide to enable editing *in trans*. To test this possibility, we targeted an mRNA encoding a potassium channel (SqKv1.2; Fig. S2*A*). As a guide, we used an RNA that contained a boxB hairpin at its center flanked by 59 nucleotides of sequence complementary to SqKv1.2 on either side. When this RNA guide was mixed with SqKv1.2 mRNA and λN–DD in vitro, we saw extensive editing in SqKv1.2 mRNA. In total, 24 of the 35 adenosines within the double-stranded region defined by the guide were edited, although to greatly different extents. As before, control reactions verified that editing required double-stranded RNA and was dependent on the λ*N*–DD-boxB interaction (Fig. S2*B*).

Our overall goal was to design guides that could drive both efficient and specific editing. However, the guide used to edit SqKv1.2 mRNA was long and seeded editing at a large number of sites. Despite this, several striking features of these data indicated that more specific guides might be possible. First, certain adenosines were edited at very high efficiencies and others were not. Notably, there was a cluster of efficiently edited adenosines at 19–21 nucleotides on the 3′ side of boxB and another at 11 nucleotides on the 5′ side. Second, adenosines close to boxB on the 3′ side were not edited at all, and those on the 5′ side were edited inefficiently. Based on these data, we hypothesized that shorter guides with the target adenosine at specific distances from boxB could promote more specific editing.

Site-Directed Editase Can Specifically Correct a Premature Termination Codon in Vitro. Our next goal was to see if we could use our system to specifically target a disease-promoting genetic mutation, both in vitro and in living cells. Ideally, we wanted to select a mutation in a protein that creates a large physiological signal so that a successful correction would be easy to identify. Mutations in ion

channels were obvious candidates. We selected the W496X mutation in the cystic fibrosis transmembrane conductance regulator (CFTR) for several reasons (24). As with many other mutations in CFTR, W496X leads to terminal cystic fibrosis, the most common genetic disease in whites. CFTR itself is an anion channel that is expressed in a variety of epithelial cells, including those within the lung. When activated by ATP and cAMP, a single CFTR channel creates a conductance of ~7–10 pS (25). Because codon 496 is located only a third of the way through the ORF, a premature termination would create a nonfunctional protein. Our aim was to develop guide RNA oligonucleotides that would specifically target only adenosine 1487 (which causes W496X) without generating unwanted mutations at other adenosines. These guides would first be tested in vitro and then extended *in cellula*.

We first generated two guides based on positional considerations gleaned from SqKv1.2 (Fig. 2*A*). The first, called guide oligonucleotide A, positioned the mutant adenosine 11 nucleotides to the 5′ of boxB (note that 5′ and 3′ refer to the target mRNA, not the guides). The second, called guide oligonucleotide B, positioned the mutant adenosine 20 nucleotides to the 3′ side. When combined with λN–DD and CFTR W496X RNA in vitro, both guides could drive correction of the mutant adenosine at ~100% efficiency. However, with each there was also nonspecific editing. With both, adenosine 1492 was also edited efficiently (M498V). Also, with guide oligonucleotide A, there was a small amount of editing at adenosine 1478 (Q493R). To make the guides more specific, oligonucleotide B was used as a model because it promoted only one off-target site. To eliminate editing at this site (M498V), we used two approaches (Fig. 2*B*). In the first, we made a new version of guide oligonucleotide B that had a mismatched cytosine adjacent to adenosine 1492. With this guide, unwanted editing at M498V was reduced from 93 to 14% without compromising editing efficiency at W496X. In addition, we made guide oligonucleotide C, which was similar to guide oligonucleotide B, but extended only four nucleotides past the target adenosine in W496X, stopping short of M498V. Thus, W496X would be in double-stranded RNA and M498V would not. With this guide, unwanted editing at M498V was completely abolished. These data show that nonspecific editing can be controlled by introducing select mismatches under the unwanted editing site or by not extending the guide oligonucleotide to include it.

For the purpose of W496X, guide oligonucleotide C was the most efficient. With concentrations of λN–DD greater than 50 nM, editing was near complete (Fig. 2*C*). In our reaction, the target CFTR RNA was present at a concentration of 2 nM and the guide oligonucleotide was present at 20 nM; with an equal concentration of λN–DD and target, editing was ~20%. Half-maximum editing occurred with a λN–DD concentration of 11 nM, which represents a molar ratio of 5.5:10:1 (λN–DD:guide oligonucleotide C:target mRNA). It should be noted that with very high concentrations of λN–DD (75 and 150 nM), off-target editing, at efficiencies from ~15–50%, could be induced at a cluster of nine adenosines downstream of the guide oligonucleotide. No off-target editing was observed at lower concentrations. No other off-target editing was seen within the 693 RT-PCR product that was sequenced for this assay. These data indicate that, for the W496X mutation, specific and efficient editing can be driven in vitro by guide oligonucleotide C.

Genetically Encoded Site-Directed Editase Can Restore CFTR Function in *Xenopus* Oocytes. To examine whether λN–DD was effective *in cellula* as well, we turned to *Xenopus* oocytes. Previous work has demonstrated that CFTR expresses robust heterologous currents in oocytes (26). An additional advantage with oocytes is that delivery is not a complicating issue because they can be directly injected with RNA. Our strategy was to inject RNA encoding λN–DD, let it express for 3 d, and then inject the same oocytes with CFTR W496X RNA and guide oligonucleotide C (Fig. 3*A*). After 3 more days oocytes were tested for CFTR expression. To be thorough, we wanted to assess correction of CFTR W496X mRNA, expression of full-length CFTR protein, and restoration of functional CFTR ionic currents. As a first step, we examined whether CFTR W496X RNA was corrected. Re-extraction of mRNA followed by RT-PCR and direct sequencing showed a corrected G peak at the mutant adenosine (Fig. 3*B*). On average, slightly more than 20% of the RNA was corrected. Importantly, no off-target editing was observed. Controls that lacked guide oligonucleotide C, λN–DD, or both showed no evidence of editing. Western blots from similar experiments also showed corrected CFTR (Fig. 3*C*). When probed with an anti-CFTR antibody that recognizes a C-terminal epitope (beyond W496X), wild-type CFTR-injected oocytes show the characteristic multiple CFTR protein bands (27). The lowest band at 127 kDa represents the unglycosylated form. The more intense upper bands represent the core glycosylated form (131 kDa) and the fully glycosylated form (160 kDa) (28). In the experimental lane, a portion of CFTR W496X was corrected, as the glycosylated forms are clearly evident. Again, controls that lacked the oligo, λN–DD, or both showed no correction. Thus, on both the level of RNA and protein, W496X was corrected by our strategy.

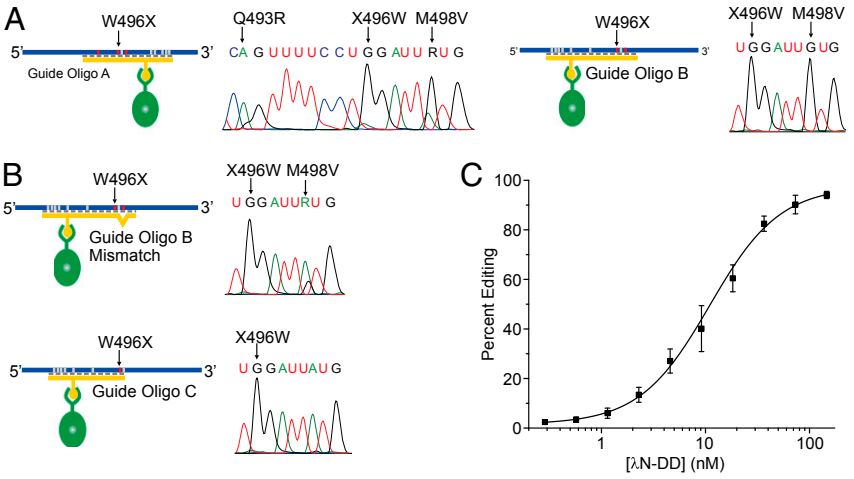

Fig. 2. Guide oligonucleotides can direct the in vitro correction of a premature termination codon that causes cystic fibrosis. (*A*) Schematics of the orientations of guide oligonucleotides A and B with respect to the W496X premature termination codon in CFTR. Editing events are indicated in red and nonedited adenosines are indicated in white. Arrows in electropherograms show the specific editing events. (*B*) Schematics for similar experiments using guide oligonucleotide B mismatch and guide oligonucleotide C and the accompanying electropherograms, $n = 5 \pm$ SEM. Editing at M498V was greatly reduced with guide oligonucleotide B mismatch and not evident with guide oligonucleotide C. Q493R was not edited with either guide (not shown), $n = 4 \pm$ SEM. (*C*) A dose–response curve for editing at X496W by guide oligonucleotide C and different amounts of λN–DD. The curve was fit with a Boltzmann equation of the form $y = E_{max} + (E_{min} - E_{max})/[1 + (X/X_0)^p]$, where E_{max} is the maximum editing percentage, E_{min} is the minimum editing percentage, X_0 is the concentration required for 50% editing, and p is a generic exponential factor. $n = 4 \pm$ SEM.

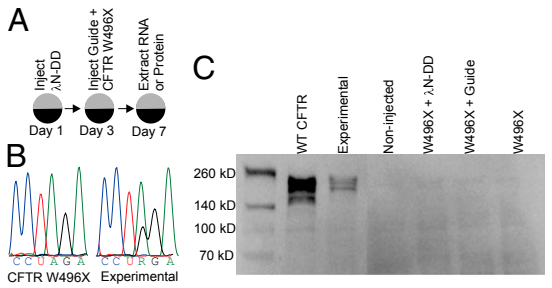

Fig. 3. Genetically encoded λN–DD can correct CFTR W496X RNA in *Xenopus* oocytes to produce full-length protein. (*A*) A schematic of the experimental design. (*B*) Electropherograms showing correction of CFTR W496X RNA (see dual peak at R). Total RNA was extracted from experimental and CFTR W496X control (no λN–DD, no guide oligonucleotide) *Xenopus* oocytes on day 7, reverse-transcribed, and used as a template to amplify the region surrounding W496X. PCR products were directly sequenced. Average percentage editing was 21.6 ± 1.8, $n = 4$ ± SEM. (*C*) Western blots from total oocyte proteins probed with an α-CFTR antibody. Equal amounts of wild-type and W496X CFTR were injected into oocytes on day 3. Blots were developed using a chemiluminescent substrate.

As a final indication of correction, we tested whether functional CFTR-mediated currents had been restored (Fig. 4). CFTR channels require ATP and cAMP to open. In oocytes, resting ATP levels are sufficient (29, 30); however, cAMP levels need to increase, and experimentally this can be accomplished by adding extracellular forskolin to stimulate adenylyl cylase activity. Fig. 4*B* shows an example of a "chart" record of membrane currents from a complete experiment recorded on a slow-time base. In this case, the oocyte was injected with wild-type CFTR, but the same approach was used for all recordings. Oocytes were held at −40 mV. At this voltage with our external solution, chloride ions will leave the cell through open CFTR channels, creating an apparent inward current. At various times during the procedure, we stepped the voltage from −80 to +40 mV in 20-mV increments (I–V) and recorded the resulting currents. These I–Vs are seen as rapid vertical deflections, and the two that we used for analysis have been labeled (1, 2). After two I–Vs, external forskolin was added, causing an inward current to develop. In Fig. 4*C* we show I–Vs before and after forskolin, recorded on a rapid-time base. Here, with wild-type CFTR, robust currents of greater than 10 μA are activated. When the same experiment was performed on oocytes injected with CFTR W496X, no currents were activated. However, when oocytes were injected with λN–DD and guide oligonucleotide C, forskolin activated large currents. Fig. 4*D* shows the average forskolin-activated conductance for experimental versus control oocytes. Data from oocytes prepared from two different frogs are presented. In both cases, enough CFTR W496X was corrected to create about 90 μS of conductance. Controls lacking λN–DD, guide oligonucleotide C, or both showed only background conductance. For these experiments, 10 times more CFTR RNA was injected into oocytes than for those used to quantify correction at W496X by RT-PCR in Fig. 3*B*. Under the present conditions, RT-PCR showed that about 15% of W496X had been corrected. In a separate set of experiments, we compared corrected W496X oocytes with wild-type CFTR to assess relative expression. When injected with 0.6 fmol of RNA, "corrected" CFTR W496X oocytes expressed approximately half of the current levels of wild-type CFTR oocytes (Fig. 4*E*). When injected with 2 times more RNA (1.18 fmol), experimental oocytes produced comparable currents to wild-type CFTR oocytes (0.6 fmol). From these results we show that the W496X premature stop codon can be corrected in a living cell by a genetically encoded λN–DD.

In the previous experiment, our system for site-directed RNA editing was not completely genetically encoded; the editase was encoded in RNA, and the guide RNA was transcribed in vitro before injecting into oocytes. To see if a fully genetically encoded version was functional, we turned to a human cell line (HEK-293T) and tested whether we could correct a version of EGFP that harbored a premature termination codon (W58X). This experiment required the transfection of three plasmids simultaneously: one encoding λN–DD and another encoding EGFP were driven by the CMV promoter. The third contained an EGFP guide RNA, very similar in design to the guide oligo C used in the CFTR experiments (the target adenosine was positioned 19 nt on the 3′ side of the boxB loop) and driven by a U6

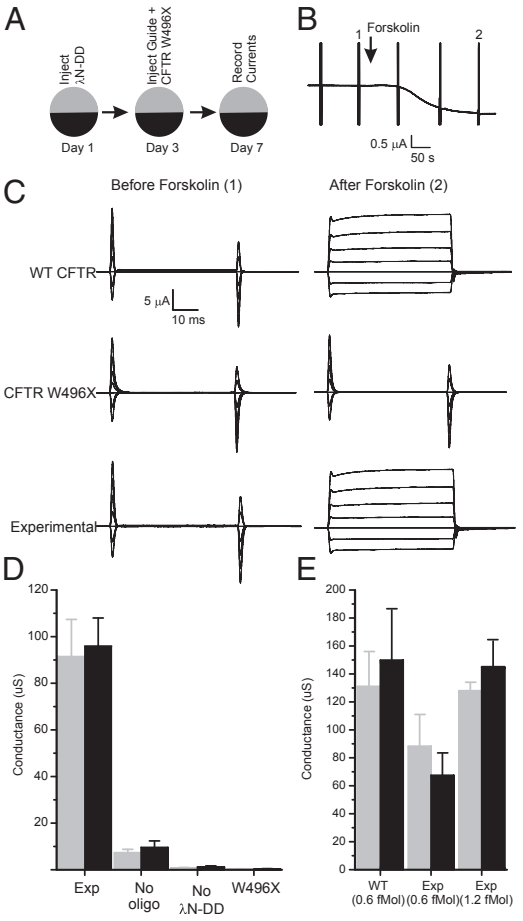

Fig. 4. Genetically encoded λN–DD can restore functional currents to oocytes injected with CFTR W496X RNA. (*A*) A schematic of the experimental design. (*B*). A current trace, recorded on a slow-time base from a voltage-clamped oocyte injected with wild-type CFTR. Current-voltage (I–V) protocols were repeated five times and can be seen as rapid vertical deflections of the trace. I–Vs marked with numbers (1, before forskolin; 2, after forskolin) were used for analysis. The others were used to monitor the stability of the recording. (*C*) Current traces resulting from voltage steps (−80 to +40 mV in 20-mV increments from a holding potential of −40 mV) presented on a rapid-time base. Transient currents in the before-forskolin traces are unsubtracted capacitance. (*D*) Forskolin-dependent conductance from whole oocytes (I–V_2 to I–V_1). Gray and black bars represent experiments repeated using different batches of oocytes removed from different frogs. Error bars are SEM. For the gray and black bars, respectively, $n = 6$ and 10 for experimental, 5 and 6 for no oligo, no λN–DD, and only W496X. (*E*) Forskolin-dependent conductance from whole oocytes injected with different amounts of wild-type (WT) CFTR or CFTR W496X with guide oligonucleotide C and λN–DD. As before, gray and black bars indicate different batches of oocytes. $n = 4$ and 5 for WT, 5 and 3 for experimental (Exp) (0.6 fMol), and 5 and 5 for Exp (1.2 fMol).

(RNA Polymerase III) promoter. This guide was able to direct 92 ± 1.2% editing ($n = 3$) at W58X in vitro as assessed by RT-PCR. As expected, wild-type EGFP-transfected HEK-293T cells gave a strong fluorescence signal, and EGFP W58X gave no detectable signal (Fig. 5*A*). EGFP W58X controls that lacked either λN–DD or the guide also yielded no detectable signal. In contrast, when EGFP W58X was transfected with both λN–DD and the guide, a strong signal was evident in many cells. A quantification of the fluorescence from individual cells revealed that the relative intensity of experimental cells was about 12% that of wild-type EGFP (see legend for Fig. 5). Direct sequences of the entire EGFP W58X cDNA revealed that ∼20% of the premature termination codon had been corrected in experimental plates (Fig. 5*B*). Moderate off-target editing was encountered at Y146S (9 ± 5.4%; $n = 3$) and K167R (38 ± 6.1%; $n = 3$). From these results we conclude that we can use genetically encoded λN–DD and guide RNA to restore function in a human cell.

Discussion

The correction of genetic mutations in mRNA is attractive for several reasons. First, compared with DNA, mRNA is accessible. Genomic DNA is sequestered in the nucleus and often tightly bound by histones. Mature mRNA, on the other hand, is in the cytoplasm. Furthermore, RNA cannot integrate into the genome and is relatively unstable, making off-target edits less of a concern than with approaches that target DNA. Another advantage for site-directed RNA editing is that it should not affect mRNA expression level. For many proteins, the precise level of expression is critical as both underexpression and overexpression can lead to disease. The MeCP2 protein is a good example where underexpression leads to Rett syndrome, and even mild overexpression can lead to autism spectrum disorders (31). Finally, many potential tools are available for RNA manipulation because there are several enzymes that can modify RNA in a base-specific manner.

To date, there have been few reports of site-directed RNA editing. Most have sought to induce endogenously expressed enzymes to correct a specific mutation by introducing a guide RNA. For example, many cellular RNAs contain pseudouridine, a *c*-glycoside isomer of the nucleoside uridine created by pseudouridine synthase. In tRNAs, specific uridines are marked for pseudouridylation by an appropriate guide RNA. When pseudouridines are present within mRNAs, they can recode a codon (32). For example, the pseudouridylated stop codons UAA and UAG are read as either serine or threonine, and UGA is read as tyrosine or phenylalanine. Targeting pseudouridylation to a premature termination codon in yeast induces read-through. A similar, albeit less specific, approach was used with endogenous ADARs. When presented with a perfect RNA duplex, ADARs will edit promiscuously. By introducing RNA oligonucleotides complementary to a premature termination codon, Woolf et al. induced endogenous ADAR to nonspecifically edit the region, including the premature termination codon, both in vitro and in *Xenopus* embryos (33). A recent study has reported a more directed approach, similar to our own (34). In it the authors coupled the catalytic domain of human ADAR1 to a guide RNA oligonucleotide using an in vitro reaction. Using this hybrid enzyme, a premature termination codon introduced into a fluorescent protein could be corrected in vitro, lending direct support to the idea that ADAR deaminase domains are fully functional on their own.

Looking forward, both the specificity and catalytic efficiency of our system for site-directed RNA editing can likely be improved by manipulating the guide or the enzyme. For this study, we were able to make a guide oligonucleotide that could direct specific editing at CFTR W496X and EGFP W58X. To extend the approach to other mutations, guide oligonucleotides must be designed empirically, with attention focused on their length, degree of complementarity, and the specific location of mismatches. Specificity may also be improved by modifying λN–DD, perhaps focusing on the length and rotational freedom of the linker between λN and the deaminase domain. In addition, it is well known that ADARs have specific preferences for the 5′ and 3′ bases that surround an editing site (35). As the molecular underpinnings of these preferences become better understood, the catalytic domain of ADAR could be manipulated to better edit adenosines in different contexts. Finally, to improve the catalytic efficiency of our system, we predict that the kinetics of the interaction between the guide oligonucleotide and its target will be important.

To realize the full potential of site-directed editing in vivo, delivery will be an important consideration. In this report, we have shown that both the guide oligonucleotide and the enzyme can be genetically encoded in plasmids and delivered via a standard transfection; however, they could probably also be delivered efficiently by viruses. In addition, transgenic animals expressing λN–DD, a guide oligonucleotide, or both could be generated to create useful models for human disease. Furthermore, recessive diseases like cystic fibrosis are often caused by alleles that carry different mutations, one of which could be corrected by editing (24, 36). At present this technique is limited to those mutations that can be corrected by recoding an A to an I; however, in principle the same approach could probably be extended to cytidine deaminases to convert C to U. Accordingly, site-directed nucleotide deamination offers the means to manipulate a wide variety of codons.

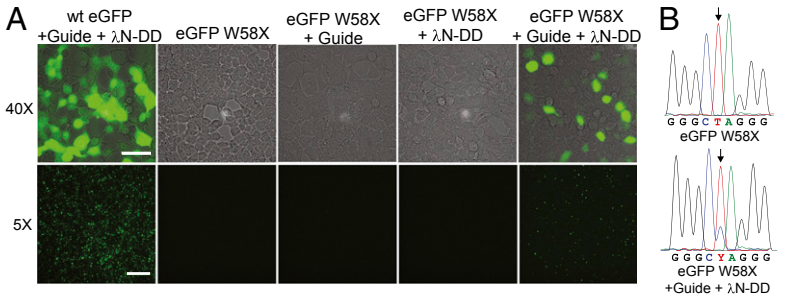

Fig. 5. Genetically encoded λN–DD and guide RNA can restore functional green fluorescence in HEK-293T cells transfected with EGFP W58X. (*A*) Images of HEK-293T cells transiently transfected with different combinations of DNA expression vectors that drive wild-type EGFP (25 ng), EGFP W58X (25 ng), EGFP Guide RNA (2 μg), and λN–DD (100 ng). The 40X images are overlays of fluorescent and differential interference contrast images. The 5X images are just fluorescent images. (Scale bar for 40X and 5X: 50 and 400 μm, respectively.) The mean relative fluorescence was measured for 200 cells from the wild-type EGFP + Guide RNA + λN–DD and the EGFP W58X + Guide RNA + λN–DD experiments. From these data the proportion of corrected EGFP W58X fluorescence to wild-type EGFP fluorescence was 12 ± 0.5%; $n = 3$. No fluorescent cells were observed in the EGFP W58X + λN–DD experiments and fewer than 10 very faint cells could be discerned in the EGFP W58X + Guide RNA. (*B*) Electropherograms of directly sequenced RT-PCR products of EGFP W58X cDNA from HEK-293T cells transfected with EGFP W58X alone or EGFP W58X + Guide RNA + λN–DD. The sequences are antisense, and the arrow points to the targeted adenosine (UAG) in the W58X premature termination codon. We estimated the correction efficiency of W58X RNA to be 20 ± 1.9%; $n = 3$. No evidence of correction was observed in the electropherograms for EGFP W58X + Guide RNA or EGFP W58X + λN–DD experiments.

Methods

Synthesis of Target RNAs, Guide RNAs, and Production of λN–DD. See *SI Methods* and Table S1.

In Vitro Editing Assays. Before the editing assay, the antisense RNA oligonucleotide or guide RNA was annealed to the RNA target using a ramp from 65 °C to 25 °C, decreasing −1 °C every 15 s. Editing assays were performed at 25 °C for 2 h with 4boxB mRNA or at 35 °C for 2 h with SqKv1.2 or CFTR mRNAs. For the data presented in Fig. 1, the assay contained 2.5 nM 4boxB RNA, 75 nM recombinant λN–DD, 2.5 nM antisense oligonucleotide, 5 mM DTT, 5 mM PMSF, 0.5 μg/μL tRNA, and 1 U/μL murine RNase inhibitor, all in Q75 [50 mM, Tris pH 7.9, 75 mM potassium chloride, and 10%(wt/vol) glycerol]. All other assays contained 2.25 nM target RNA, 75 nM recombinant λN–DD, 20 nM guide RNA oligonucleotide, 5 mM DTT, 5 mM PMSF, 0.5 μg/μL tRNA, and 1 U/μL murine RNase inhibitor, all in Q200 (same as Q75 except 200 mM potassium glutamate was substituted for the 75 mM potassium chloride). For blocking control assays, we added 7.5 μM boxB or boxB mutant oligonucleotide or 250 μM λN peptide. λN peptide was purchased from New England Peptide. BoxB and mutated boxB RNAs (G8A, A10C) were synthesized commercially.

Estimation of Editing Efficiency. After editing in vitro, cDNA was synthesized using the AccuScript High-Fidelity RT-PCR Kit (Agilent Technologies). After amplifying the cDNA by PCR, products were sent for direct sequencing. Quantification of editing percentages was performed by comparing the deoxycytidine/deoxythymidine peak heights in the antisense strand according to published protocols (37, 38).

Injection of *Xenopus* Oocytes. On day 1, oocytes were injected with 368 fmol of λN–DD. After 3 d, they were reinjected with 1 pmol (electrophysiology) or 2.8 pmol (RNA or total protein extraction experiments) of guide RNA C and the following amounts of CFTR W496X RNA: 1.18 fmol for electrophysiology experiments, 0.118 fmol for RNA extraction, or 11.8 fmol for total protein extraction.

Extraction of RNA. See *SI Methods*.

Preparation of Total Proteins. See *SI Methods*.

Western Blots. Blots were performed using total protein as described above. Samples were run on a 4–20%(wt/vol) gradient gel and transferred onto PVDF membranes. Membranes were blocked with SuperBlock T20 (TBS) Blocking Buffer (Thermo Scientific) and probed with a primary antibody α-CFTR at 1:500 (clone M3A7; Millipore), followed by a HRP-linked goat anti-mouse secondary at 1:5,000. The M3A7 antibody recognizes human CFTR amino acids 1365–1395, which are close to the C terminus. All incubations were performed in blocking buffer. Membranes were washed with Tris buffered saline with Tween 20, developed with an enhanced chemiluminescent substrate (SuperSignal West Femto, Thermo Scientific), and imaged using a KODAK Image Station 4000R.

Electrophysiology. See *SI Methods*.

Expression of EGFPs in HEK-293T Cells and Analysis of Fluorescence. See *SI Methods*.

ACKNOWLEDGMENTS. We thank Dr. Carol Wilusz for useful discussions on λN and boxB and for providing clones. We also thank Drs. J. Adelman and Mary O'Connell for providing clones. This work was supported by National Institutes of Health (NIH) Grants 2 U54 NS039405-06 and R01 NS064259NIH (to J.J.C.R.); National Science Foundation Grants IBN-0344070 and HRD-1137725 (to J.J.C.R.); and National Institute on Drug Abuse Grant DA023444 and NIH Grant 1P30NS069258 (to G.A.Y.). Infrastructure support was provided in part by grants from the National Center for Research Resources (2G12RR003051) and the National Institute on Minority Health and Health Disparities (8G12MD007600).

1. Bass BL, Weintraub H (1987) A developmentally regulated activity that unwinds RNA duplexes. *Cell* 48(4):607–613.
2. Bass BL, Weintraub H (1988) An unwinding activity that covalently modifies its double-stranded RNA substrate. *Cell* 55(6):1089–1098.
3. Kim U, Wang Y, Sanford T, Zeng Y, Nishikura K (1994) Molecular cloning of cDNA for double-stranded RNA adenosine deaminase, a candidate enzyme for nuclear RNA editing. *Proc Natl Acad Sci USA* 91(24):11457–11461.
4. Melcher T, et al. (1996) A mammalian RNA editing enzyme. *Nature* 379(6564):460–464.
5. O'Connell MA, Gerber A, Keegan LP (1998) Purification of native and recombinant double-stranded RNA-specific adenosine deaminases. *Methods* 15(1):51–62.
6. O'Connell MA, Gerber A, Keller W (1997) Purification of human double-stranded RNA-specific editase 1 (hRED1) involved in editing of brain glutamate receptor B pre-mRNA. *J Biol Chem* 272(1):473–478.
7. Basilio C, Wahba AJ, Lengyel P, Speyer JF, Ochoa S (1962) Synthetic polynucleotides and the amino acid code, V. *Proc Natl Acad Sci USA* 48(4):613–616.
8. Rosenthal JJ, Seeburg PH (2012) A-to-I RNA editing: Effects on proteins key to neural excitability. *Neuron* 74(3):432–439.
9. Bhalla T, Rosenthal JJ, Holmgren M, Reenan R (2004) Control of human potassium channel inactivation by editing of a small mRNA hairpin. *Nat Struct Mol Biol* 11(10):950–956.
10. Burns CM, et al. (1997) Regulation of serotonin-2C receptor G-protein coupling by RNA editing. *Nature* 387(6630):303–308.
11. Colina C, Palavicini JP, Srikumar D, Holmgren M, Rosenthal JJ (2010) Regulation of Na+/K+ ATPase transport velocity by RNA editing. *PLoS Biol* 8(11):e1000540.
12. Sommer B, Köhler M, Sprengel R, Seeburg PH (1991) RNA editing in brain controls a determinant of ion flow in glutamate-gated channels. *Cell* 67(1):11–19.
13. Nishikura K (2010) Functions and regulation of RNA editing by ADAR deaminases. *Annu Rev Biochem* 79:321–349.
14. Herb A, Higuchi M, Sprengel R, Seeburg PH (1996) Q/R site editing in kainate receptor GluR5 and GluR6 pre-mRNAs requires distant intronic sequences. *Proc Natl Acad Sci USA* 93(5):1875–1880.
15. Higuchi M, et al. (1993) RNA editing of AMPA receptor subunit GluR-B: A base-paired intron-exon structure determines position and efficiency. *Cell* 75(7):1361–1370.
16. Macbeth MR, et al. (2005) Inositol hexakisphosphate is bound in the ADAR2 core and required for RNA editing. *Science* 309(5740):1534–1539.
17. Chattopadhyay S, Garcia-Mena J, DeVito J, Wolska K, Das A (1995) Bipartite function of a small RNA hairpin in transcription antitermination in bacteriophage lambda. *Proc Natl Acad Sci USA* 92(9):4061–4065.
18. Austin RJ, Xia T, Ren J, Takahashi TT, Roberts RW (2002) Designed arginine-rich RNA-binding peptides with picomolar affinity. *J Am Chem Soc* 124(37):10966–10967.
19. Keegan LP, Rosenthal JJ, Roberson LM, O'Connell MA (2007) Purification and assay of ADAR activity. *Methods Enzymol* 424:301–317.
20. Palavicini JP, O'Connell MA, Rosenthal JJ (2009) An extra double-stranded RNA binding domain confers high activity to a squid RNA editing enzyme. *RNA* 15(6):1208–1218.
21. Gehring NH, et al. (2005) Exon-junction complex components specify distinct routes of nonsense-mediated mRNA decay with differential cofactor requirements. *Mol Cell* 20(1):65–75.
22. Cilley CD, Williamson JR (1997) Analysis of bacteriophage N protein and peptide binding to boxB RNA using polyacrylamide gel coelectrophoresis (PACE). *RNA* 3(1):57–67.
23. Tan R, Frankel AD (1995) Structural variety of arginine-rich RNA-binding peptides. *Proc Natl Acad Sci USA* 92(12):5282–5286.
24. Balassopoulou A, Papadakis M, Loukopoulos D (1994) A novel nonsense mutation identified in the first nucleotide binding fold of the CFTR gene in a Greek patient. *Hum Mol Genet* 3(10):1887–1888.
25. Egan M, et al. (1992) Defective regulation of outwardly rectifying Cl- channels by protein kinase A corrected by insertion of CFTR. *Nature* 358(6387):581–584.
26. Bear CE, et al. (1991) Cl- channel activity in Xenopus oocytes expressing the cystic fibrosis gene. *J Biol Chem* 266(29):19142–19145.
27. Gregory RJ, et al. (1990) Expression and characterization of the cystic fibrosis transmembrane conductance regulator. *Nature* 347(6291):382–386.
28. Cheng SH, et al. (1990) Defective intracellular transport and processing of CFTR is the molecular basis of most cystic fibrosis. *Cell* 63(4):827–834.
29. Gribble FM, et al. (2000) A novel method for measurement of submembrane ATP concentration. *J Biol Chem* 275(39):30046–30049.
30. Venglarik CJ, Schultz BD, Frizzell RA, Bridges RJ (1994) ATP alters current fluctuations of cystic fibrosis transmembrane conductance regulator: Evidence for a three-state activation mechanism. *J Gen Physiol* 104(1):123–146.
31. Peters SU, et al. (2013) The behavioral phenotype in MECP2 duplication syndrome: A comparison with idiopathic autism. *Autism Res* 6(1):42–50.
32. Karijolich J, Yu YT (2011) Converting nonsense codons into sense codons by targeted pseudouridylation. *Nature* 474(7351):395–398.
33. Woolf TM, Chase JM, Stinchcomb DT (1995) Toward the therapeutic editing of mutated RNA sequences. *Proc Natl Acad Sci USA* 92(18):8298–8302.
34. Stafforst T, Schneider MF (2012) An RNA-deaminase conjugate selectively repairs point mutations. *Angew Chem Int Ed Engl* 51(44):11166–11169.
35. Lehmann KA, Bass BL (2000) Double-stranded RNA adenosine deaminases ADAR1 and ADAR2 have overlapping specificities. *Biochemistry* 39(42):12875–12884.
36. Schwarz MJ, et al. (1995) Cystic fibrosis mutation analysis: Report from 22 U.K. regional genetics laboratories. *Hum Mutat* 6(4):326–333.
37. Eggington JM, Greene T, Bass BL (2011) Predicting sites of ADAR editing in double-stranded RNA. *Nat Commun* 2:319.
38. Rinkevich FD, Schweitzer PA, Scott JG (2012) Antisense sequencing improves the accuracy and precision of A-to-I editing measurements using the peak height ratio method. *BMC Res Notes* 5:63.

Supporting Information

Montiel-Gonzalez et al. 10.1073/pnas.1306243110

SI Methods

Sequences Used. Specific sequences used in this work were the following: The sequence of the λN peptide was MNARTRRRERRAEKQAQWKAAN. The sequence used for the deaminase domain of hADAR2 comprised amino acids 299–701 of GenBank accession no. U82120. The sequence for 4boxB RNA target was UAAGCUCGCUUUCUUGCUGUCCAAUUUCUAUUAAAGGUUCCUUUGUUCCCUAAGCUCGACCAAAGGUUCCUUUGUGGCCCUGAAAAAGGGCCAAAUUGGUGGCUGGUGUGGCUAAUGCCCUAUGGCCCUGAAAAAGGGCCACUGGAGGAUAUUCAUGCACUCGACCAAAGGUUCCUUUGUGGCCCUGAAAAAGGGCCAAAUUGGUGGCUGGUGUGGCUAAUGCCCUAUGGCCCUGAAAAAGGGCCACUGGAGGAUAUUCAUGCACUCGAGUACUAAACUGGGGGAUAUUAUGAAGGGCCUUGAGCAUCUGGAUUCUGCCUAAU (boxB sequences are underlined).

The sequence used to synthesize the guide oligo SqKv1.2 for Figs. S1 and S2 was **TAATACGACTCACTATAGGGAGA**CGATTAGTTAGAGTTTTCCGTATTTTCAAGCTCTTGGCCCTGAAAAAGGGCCCTAGACATTCTAAAGGATTACAAATACTCGGCCAG (T7 tag in boldface type; boxB is underlined).

Expression of EGFP and EGFP W58X in HEK-293T Cells. HEK-293T cells were maintained in Dulbecco's Modified Eagle's Medium supplemented with 10%(vol/vol) FBS, 1% penicillin–streptomycin solution, and 1 mM sodium pyruvate. For each transfection, 6 × 105 cells were seeded in a 35-mm glass-bottom dish and the next day was exposed to plasmid DNA and Effectene Transfection Reagent (Qiagen) according to the supplied protocol. EGFP and EGFP W58X, both driven by the CMV promoter and cloned into the plasmid pJPA7 were kindly provided by J. Adelman (Vollum Institute, Portland, OR). DNA sequence encoding the EGFP W58X guide RNA was driven by an RNA polymerase III promoter in the U6 RNAi Entry Vector (Invitrogen). λN-DD was also driven by the CMV promoter in the vector pcDNA3.1(−). The following amounts of each plasmid were used for each transfection: EGFP or EGFP W58X (25 ng), λN-DD (100 ng), and EGFP W58X guide (2 μg). Cells were analyzed 36 h posttransfection.

Detection and Analysis of EGFP Fluorescence. Fluorescence imaging was performed using a Nikon Ti-E microscope with a Plan Apo lambda 40× or 5× N.A. 0.95 objective and a 100-W halogen lamp. Images were acquired using an iXonEM+ DU897 back-illuminated EMCCD camera (Andor) and NIS elements software. The camera was operated in the linear range during all of the imaging sessions. Sample temperature was controlled at 37 °C. Cells were imaged in serum-free OptiMEM (Life Technologies) supplemented with 20 mM Hepes (pH 7.4). ImageJ Fiji software (http://fiji.sc/Fiji) was used to analyze images. For positive control and experimental transfections, 200 fluorescent cells were selected at random, and the integrated fluorescence density was measured in a standard area. Background values from nonfluorescent cells were subtracted from each value.

Extraction of RNA. Cystic fibrosis transmembrane conductance regulator (CFTR) W496X mRNA samples were extracted from 10 *Xenopus* oocytes using the RNaqueous Kit (Ambion Life Technologies). This same kit was used for the extraction of RNA from HEK-293T cells. cDNA was synthesized using RT-primer 5 and amplified by PCR using primers 6 and 7 (Table S1). The final product was directly sequenced using primer 8.

Preparation of Total Proteins. For the extraction of total oocyte proteins, we followed a protocol kindly provided by M. Holmgren (National Institute of Neurological Disorders and Stroke, Bethesda, MD). Forty oocytes were washed 3× with 2 mL of ND96 and another 6× with 1 mL of ND96 and then lysed with 800 μL of ice-cold Triton X-100 lysis buffer (1% Triton X-100, 100 mM NaCl, 20 mM Tris·HCl, 10 μL/mL protease inhibitors mixture by Thermo Scientific). Samples were centrifuged at 13,000 × *g* for 2 min at 4 °C. For Western Blots of total proteins, we removed 80 μL of the supernatant.

Electrophysiology. Oocytes were prepared as described (1). CFTR expression was assessed in whole oocytes using a conventional two-microelectrode voltage clamp amplifier (GeneClamp 500B, Axon Instruments). Analog signals were filtered at 1 kHz and digitized using an Innovative Integrations SBC6711 A/D converter. GPATCH software, kindly provided F. Bezanilla (University of Chicago, Chicago), was used to control voltage. Records on a slow-time scale were collected using a MiniDigi 1A board and AxoScope 9.0 software (Axon Instruments). Oocytes were held at −40 mV and perfused with ND-96 solution. CFTR currents were activated by perfusing ND-96 with 40 μM forskolin. Current-voltage protocols consisted of stepping the membrane potential from −80 to +40 mV for 50 ms in 20-mV increments. Whole-oocyte CFTR slope conductance was estimated by subtracting current-voltage patterns before and after the addition of forskolin.

Synthesis of Target RNAs, Guide RNAs, and Production of λN-DD. Target RNAs were synthesized using AmpliScribe T7 or the T3 High Yield Transcription Kit (Epicentre Biotechnologies). 4boxB plasmid was provided by the Carol Wilusz laboratory (Colorado State University, Fort Collins, CO). CFTR DNA was provided from David Gadsby (The Rockefeller University, New York). The Quikchange Lightning Site-directed Mutagenesis kit (Stratagene) was used for site-directed mutagenesis. The Guide RNA complementary to SqKv1.2 was synthesized from a SqKv1.2 construct that had a boxB hairpin inserted at position 1041. CFTR guide RNAs were synthesized with either the MessageMuter shRNA Production Kit (Epicentre Biotechnologies) or by designing T7-tagged DNA oligonucleotides for in vitro transcription using the mScript mRNA Production System (Epicentre Biotechnologies).

To make recombinant λN-DD protein, the amino-terminus of the deaminase domain was fused to the carboxy-terminus of the λN peptide using a two-step PCR protocol. We first amplified λN with oligonucleotides 1 and 2 (Table S1) using a plasmid that contained the λN DNA sequence. The deaminase domain was amplified with oligonucleotides 3 and 4 from human ADAR2. These two products were then fused by mixing the PCR products and amplifying with oligonucleotides 1 and 4 (Table S1). All PCR reactions were performed using Phusion DNA Polymerase (New England Biolabs).

1. Galarza-Muñoz G, Soto-Morales SI, Holmgren M, Rosenthal JJ (2011) Physiological adaptation of an Antarctic Na+/K+-ATPase to the cold. *J Exp Biol* 214(Pt 13):2164–2174.

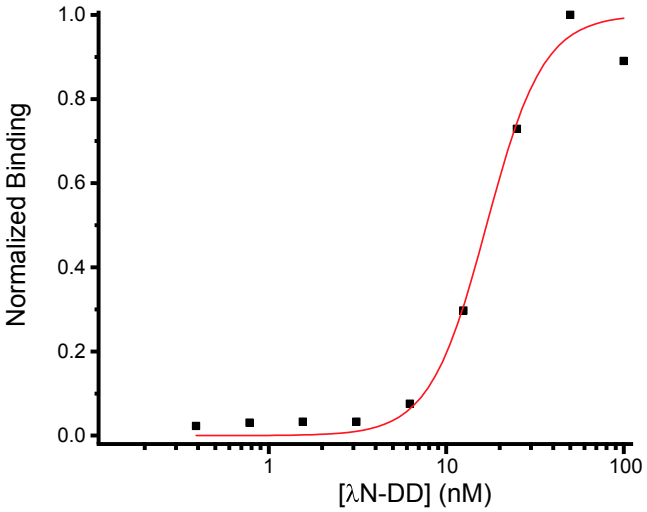

Fig. S1. Recombinant λN-DD binds boxB RNA. To determine the binding affinity between λN-DD and the boxB guide RNA, we performed filter binding assays (1). We transcribed guide RNA SqKv1.2 with T7 RNA polymerase in the presence of 35 μCi of [α-^{32}P]UTP (3,000 Ci/mmol; 1 Ci = 37 GBq), 1X T7 buffer, rCGU mix (3.3 mM final concentration each), 2 mM rA, 0.1 M DTT, RNase Inhibitor. The binding reaction contained Q200 potassium glutamate (K-Glu) buffer, pH 7 [200 mM K-Glu, 10 mM Tris glutamate, pH 7, and 20% (wt/vol) glycerol]; in addition, we added 1 mM DTT, 0.5 mM PMSF, 0.5 μg/μL tRNA, and 1 U/μL RNase inhibitor in a volume of 30 μL. The reaction was incubated at 37 °C for different times (5, 10, 15, 30, 60, 120, and 180 min) to determine the time when the reaction reached equilibrium. Binding assays were performed by adding 5,000 cpm of guide RNA and different dilutions of λN-DD (100, 50, 25, 12.5, 6.25, 3.125, 1.56, 0.78, 0.39, 0.19, 0.09, 0.04, and 0.02 nM). To determine the K_d, fraction-bound RNA was plotted versus different concentrations of λN-DD and fit the graph to a Boltzmann function of the formula $F = [\lambda N - \mathrm{DD}]^n/([\lambda N - \mathrm{DD}]^n + \mathrm{KD}^n)$, where F refers to the fraction of bound RNA.

1. Chen CX, et al. (2000) A third member of the RNA-specific adenosine deaminase gene family, ADAR3, contains both single- and double-stranded RNA binding domains. *RNA* 6(5): 755–767.

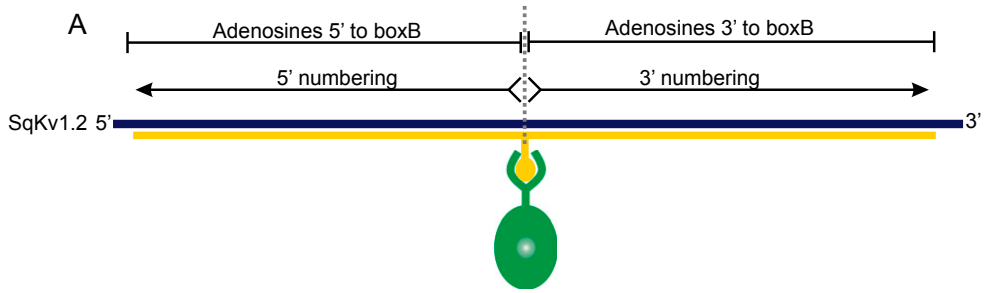

B

Adenosines 5'	Editing % Experimental	Editing % Excess mutant boxB	Editing % Excess boxB	Editing % Excess λN	Editing % No λN-DD	Editing % No RNA oligo
2	20 ± 0.8	19 ± 2.7	ND	ND	ND	12 ± 1.5
8	18 ± 0.9	18 ± 3.2	ND	ND	ND	ND
9	ND	ND	ND	ND	ND	ND
11	97 ± 0.04	96 ± 1	ND	11± 0.5	ND	8 ± 0.5
18	29 ± 0.7	30 ± 1.7	ND	ND	ND	ND
19	91 ± 0.7	89 ± 2.4	ND	ND	ND	ND
25	65 ± 1.1	61 ± 6.8	ND	ND	ND	ND
28	17 ± 1.6	17 ± 2	ND	5± 1.4	ND	17 ± 0.5
40	ND	ND	6 ± 0.3	ND	6 ± 0.6	ND
52	ND	ND	ND	ND	ND	ND

Adenosine 3'	Editing % Experimental	Editing % Excess mutant boxB	Editing % Excess boxB	Editing % Excess λN	Editing % No λN-DD	Editing % No RNA oligo
1	ND	ND	ND	ND	ND	ND
3	ND	ND	ND	ND	8 ± 3.2	7 ±1
9	ND	ND	ND	ND	ND	ND
10	ND	ND	ND	ND	ND	ND
11	ND	ND	ND	ND	ND	ND
12	ND	ND	ND	ND	ND	ND
14	88 ± 1.2	85 ± 4.2	ND	ND	ND	ND
18	ND	ND	ND	ND	ND	ND
19	95 ± 0.5	95 ± 1.6	ND	ND	ND	6 ±2
20	97 ± 0.6	97 ± 0.8	ND	ND	ND	ND
21	91 ± 1	91 ± 1.3	ND	ND	ND	ND
26	46 ± 1.3	42 ± 5.3	ND	ND	ND	ND
27	68 ± 1	65 ± 4.8	ND	ND	ND	ND
30	73 ± 0.5	71 ± 3.8	ND	ND	ND	ND
31	77 ± 0.4	78 ± 2.3	ND	ND	ND	ND
35	15 ± 1	14 ± 3.4	ND	ND	ND	ND
36	42 ± 1.7	52 ± 9.5	ND	ND	ND	ND
39	15 ± 0.1	15 ± 3.3	ND	ND	ND	ND
44	91 ± 0.1	91 ± 2.5	ND	ND	ND	14 ±4
45	92 ± 0.4	91 ± 1.6	ND	10 ±1.3	ND	12 ±0.2
47	ND	ND	ND	ND	ND	ND
48	19 ± 0.7	19 ± 2.2	ND	ND	ND	ND
53	87 ± 1	88 ± 4.2	ND	ND	ND	7 ±3
54	91 ± 0.9	89 ± 3.1	ND	ND	ND	15 ±4
58	13 ± 0.8	12 ± 1.8	ND	ND	ND	ND

Fig. S2. Recombinant λN-DD can edit *in trans*. (*A*) A schematic of the experimental design. After incubating SqKv1.2 RNA (blue) with a long complementary guide oligonucleotide (133 nt) with a boxB hairpin inserted at its center (yellow) and recombinant λN-DD (green), RT-PCR revealed editing at select adenosines. (*B*) Editing percentages in experimental and control reactions at specific adenosines on the 5′ and 3′ sides of the boxB loop (see *A* for orientation). Numbering indicates an adenosine's distance in nucleotides from the boxB insertion. Note that this is a nucleotide position and does not indicate the number of adenosines from the boxB insertion. Because numbering is relative to the boxB insertion, 5′ adenosines increase from right to left, and 3′ adenosines increase from left to right. $n = 3 \pm$ SEM. Any editing below 5% was considered background. ND, none detected.

Table S1. DNA and RNA oligonucleotides used in this work

Oligonucleotide no.	Oligonucleotide name	Sequence	Target sequence	Associated text figure	Description
1	MF1	AGACTAGTAAACGCACGAACACGACGACGT	1–21 λN	NA; used to create λN	Fwd primer to amplify λN peptide; contains 5′ Spe I site
2	MF2	AGATGGCGTCTGATCCAAGTGCAAGTTTGCAGCTTT CCATTGAGC	43–63 λN; 895–918 human ADAR2	NA; used to create λN	Rev primer to amplify λN peptide; also contains sequence to the 5′ end of human ADAR 2 deaminase domain
3	MF3	TTGCACTTGGATCAGACGCCATCT	895–918 human ADAR2	NA; used to create λN	Fwd primer to amplify 5′ end of human ADAR 2 deaminase domain
4	MF4	AGACTAGTGGCGTGAGTGAGAACTGGTC	2083–2102 human ADAR2	NA; used to create λN	Rev primer to amplify 3′ end of human ADAR 2 deaminase domain
5	CFTR22	CGGACAATTTCCCTCTCAGCAGTGGCCAGGAGACAGGAGCATCTCC	2018–2037 CFTR	Figs. 2 and 3	RT primer for CFTR cDNA; contains a 5′ ACT5 (primer 7) tag
6	CFTR19	GAAAGAGGACAGTTGTTGGCGG	1345–1366 CFTR	Figs. 2 and 3	Fwd PCR primer to amplify CFTR cDNA
7	ACT5	CGGACAATTTCCCTCTCAGCAGTGG	Primer tag	Figs. 2 and 3	Rev PCR primer to amplify CFTR cDNA
8	CFTR9	Gagaaacggtgtaaggtctcag	1988–2009 CFTR	Figs. 2 and 3	Rev primer to sequence CFTR PCR fragment
9	4boxB AS RNA	5′ACAAAGGAACCUUUGGUCGAGUGCAUG3′	55–75/154–180 4boxB	Fig. 1	Antisense RNA oligonucleotide complementary to two sites in 4boxB RNA
10	BoxB RNA	5′UGGCCCUGAAAAAGGGCCA3′	NA	Fig. 1 and Fig. S2	BoxB RNA oligonucleotide for blocking controls
11	BoxB mutant	5′UGGCCCU***A***A***C***AAAGGGCCA3′	NA	Fig. 1 and Fig. S2	Mutated BoxB RNA oligonucleotide for blocking controls. Boxes indicate mutant positions.
12	Guide RNA SqKv1.2-BoxB	5′GUCGCUUGCGAUUCUUAGGGUCAUUCGAUUAGUUAGAGUUU UCCGUAUUUUCAAGCUCUUGGCCCUGAAAAAGGGCCCUAGAC AUUCUAAAGGAUUACAAAUACUCGGCCAGACCCUCAAAGCCA GCAUGAGG-3′	507–613 SqKv1.2	Fig. S2	Sense RNA oligonucleotide complementary to SqKv1.2 AS nt 507–613 but bisected with a boxB hairpin (underlined)
13	Guide DNA A	5′TAATACGACTCACTATAGGGAGACTTTAATGGTGCGGCCCTGAA AAAGGGCCGCATAATCTAGGAAAACTGAGAACAGCC-3′	1470–1495 and 1499–1510 CFTR	Fig. 2	Sense DNA oligonucleotide used to synthesize guide A RNA for CFTR W496X in vitro editing assay; has 5′ T7 tag.
14	Guide DNA A (AS)	5′GGCTGTTCTCAGTTTTCCTAGATTATGCGGCCCTTTTTCAGGGCCG CACCATTAAAGTCTCCCTATAGTGAGTCGTATTA3′	1470–1495 and 1499–1510 CFTR	Fig. 2	Antisense DNA oligonucleotide used to synthesize guide A RNA for CFTR W496X in vitro editing assay; has 5′ T7 tag
15	Guide AS DNA B	5′**GG**GTGGAAGAATTTGGCCCTTTTTCAGGGCCTCTGTTCTCAGTTTT CCTAGATTATGCCTGGC**TATAGTGA**-3′	1454–1465 and 1469–1500 CFTR	Fig. 2	Sense DNA oligonucleotide used to synthesize guide B RNA using MessageMuter shRNA production kit (Epicentre). Extra nucleotides required by the kit are in boldface type.
16	Guide AS DNA B-mismatch	5′**GG**GTGGAAGAATTTGGCCCTTTTTCAGGGCCTCTGTTCTCAGTTTT CCTAGATTCTGCCTGGC**TATAGTGA**3′	1454–1465 and 1469–1500 CFTR	Fig. 2	Sense DNA oligonucleotide used to synthesize guide B-mismatch RNA using MessageMuter shRNA production kit (Epicentre). Extra nucleotides required by the kit are in boldface type.
17	Guide DNA C	5′TAATACGACTCACTATAGGGAGAAATCTAGGAAAACTGAGAAC AGAGGCCCTGAAAAAGGGCCAAATTCTTCCACCC-3′	1452–1465 and 1469–1491 CFTR	Figs. 2, 3, 4	Sense DNA oligonucleotide used to synthesize guide C RNA for CFTR W496X in vitro editing assay; has 5′ T7 tag.

Table S1. Cont.

Oligonucleotide no.	Oligonucleotide name	Sequence	Target sequence	Associated text figure	Description
18	Guide DNA C (AS)	5′GGGTGGAAGAATTTGGCCTTTTTCAGGGCCTCTGTTCTCAGTTT TCCTAGATTTCTCCCTA TAGTGAGTCGTATTA3′	1452–1465 and 1469–1491 CFTR	Figs. 2, 3, and 4	Antisense DNA oligonucleotide used to synthesize guide C RNA for CFTR W496X in vitro editing assay; has 5′ T7 tag
19	BoxB RT	GGCGTACAGGGACAGAACAGCTTGGGGCAGAATCCAGATGCTC	302–319 4boxB	Fig. 1	RT primer for making 4boxB cDNA; contains a 5′ ACT2 (primer 24) tag
20	BoxB1	TAAGCTCGCTTTCTTGCTGTCC	1–22 4boxB	Fig. 1	Fwd PCR primer to amplify 4boxB cDNA
21	BoxB2	ATTAGGCAGAATCCAGATGCTC	302–323 4boxB	Fig. 1	Rev primer to sequence 4boxB
22	Kv1.2 RT ACT2	GGCGTACAGGGACAGAACAGCTTGGGGGAGGAGGTGGTGGAG ATGAG	1504–1522 SqKv1.2	Fig. S2	RT primer for making SqKv1.2 cDNA; contains a 5′ ACT2 (primer 24) tag
23	SqKv1.2–11	GGGCAGGGTCTCAAGGCAG	874–892 SqKv1.2	Fig. S2	Fwd PCR primer to amplify SqKv1.2 AS
24	ACT2	GGCGTACAGGGACAGAACAGCTTGG	Primer tag	Fig. 1 and Fig. S2	Rev PCR primer to amplify 4boxB and SqKv1.2. AS
25	SqKv1.2–5	CCTTGGGAACCGTTATCGCTG	642–662 SqKv1.2	Fig. S2	Reverse sequencing primer for SqKv1.2 AS
26	U6EGFPAdl#1 sense	**CACC**GGGCCAGGGCACGGGCAGCTTGCGGCCCTGAAAAAGGGCC TGGTGCAGATGAAC		Fig. 5	Sense DNA oligonucleotide encoding guide DNA for EGFP W58X. This was cloned into the BLOCK-iT U6 RNAi Entry Vector Kit (Invitrogen). Restriction site overhangs required by the kit are in boldface type.
27	U6EGFPAdl#1 antisense	**AAAA**GTTCATCTGCACCAGGCCCTTTTTCAGGGCCGCAAGCTGCC CGTGCCCTGGCCC	155–177 boxB 138–151nt	Fig. 5	Antisense DNA oligonucleotide complementary to oligo 26. Restriction site overhangs required by the kit are in boldface type.
28	EGFP Fwd Adelman	ATGGTGAGCAAGGGCGAGGAGC	1–22 EGFP RNA	Fig. 5	PCR primer to amplify EGFP cDNA
29	EGFP Rev Adelman	CAGCTCGTCCATGCCGAGAGTG	690–711 EGFP RNA	Fig. 5	PCR primer to amplify EGFP cDNA; also used as a sequencing primer

Underlined sequences identify the boxB hairpin. In boldface type are the sequences required for the MessageMuter shRNA Production Kit (Epicentre; oligos 15 and 16) or the Block-iT U6 RNAi Entry Vector Kit (Invitrogen). Boldface italic nucleotides represent the mutations made in the boxB hairpin to disrupt its interaction with the λN peptide. Oligonucleotides 10 and 11 were tagged at the 5′ end with hexachlorofluorescein phosphoramidite. Guide oligonucleotides nos. 13, 14, 17, and 18 are tagged with a T7 sequence. Fwd, sense strand oligonucleotide; Rev, antisense strand oligonucleotide; NA, not applicable.